Advanced and Sustainable Technologies
ASET
E-ISSN 2976-2294
Volume 4, No 2, December 2025 [96-121]

Development of 3D Numerical Model to Investigate Land Reclamation Impact around Penang Island

Anas Abdul Rahman[1]*, Arif Muhamad[1] and Ayu Abdul Rahman[2]

[1] Mechanical Engineering Programme, Faculty of Mechanical Engineering & Technology, Universiti Malaysia Perlis (UniMAP), Pauh Putra Main Campus, 02600 Arau, Perlis, Malaysia.
[2]Department of Mathematics and Statistics, School of Quantitative Sciences, Universiti Utara Malaysia, 06010 UUM, Sintok, Kedah, Malaysia.

Received 9 September 2025, Revised 19 September 2025, Accepted 13 October 2025

ABSTRACT

Land reclamation in Malaysia, particularly in states such as Kedah, Penang, Perak, Johor, and Melaka, has significant consequences for marine biodiversity and coastal communities. It alters hydrodynamic patterns, increasing siltation in waterways and threatening the marine ecosystem, the livelihoods of fishermen, and the socio-economic well-being of residents. This study focuses on the Seri Tanjung Pinang (STP) reclamation project in Penang Island, Malaysia, which has raised concerns about its environmental and socio-economic impacts. To evaluate the hydrodynamic response of the surrounding waters, a three-dimensional numerical model was developed using TELEMAC3D. Unlike previous studies that often relied on coarser grids, this research systematically examines the effect of mesh resolution on tidal flow predictions, thereby improving the reliability of the model in capturing local-scale dynamics around reclamation sites. The results reveal pronounced hydrodynamic changes induced by the STP reclamation, with tidal velocities increasing by approximately 13–19% at most monitored points, while one southern location experienced a decrease of about 8%. These changes indicate higher potential for siltation in nearby waterways, driven by stronger tidal velocities and reduced flood tidal currents. Such alterations are likely to affect fisheries, recreational activities, and critical habitats. The findings underscore the importance of using higher-resolution numerical models to accurately assess reclamation impacts and provide more robust input for Environmental Impact Assessments (EIA) and policymaking.

Keywords: Coastal management, Current flow, Mesh propagation, Tidal model, Telemac3D.

1. INTRODUCTION

In the last few decades, Malaysia has been experiencing rapid economic growth within the ASEAN region. It has a lengthy coastline along Peninsular Malaysia's west coast, spanning approximately 800 km from Perlis to Johor, encompassing the northern to southern regions of the country. Among Malaysia's islands, Penang Island is the fourth largest, covering an area of 295 km2 (114 square miles) [1]. It is situated at the Straits of Malacca, as depicted in Figure 1(a), and is separated from Sumatra Island. With an estimated population of 678,000 people, Penang Island, or Pulau Pinang, is the most populous island in Malaysia and is connected to the mainland by two Penang Bridges. Renowned for its scenic beauty and well-developed city, Penang has experienced significant economic growth, leading to its rapid development. Consequently, the island is facing a challenge of limited land availability due to the increasing demand for urban development, infrastructure, and the growing population of the state. To address this issue, the Department of

*Corresponding author: anasrahman@unimap.edu.my

Environmental Impact Assessment (DEIA) approved the Tanjung Tokong Land Reclamation Project in April 2014 [2]. Figures 1(b), (c), and (d) highlight the location and view of the Tanjung Tokong Land Reclamation Project, which is situated in the north-east region of Penang Island.

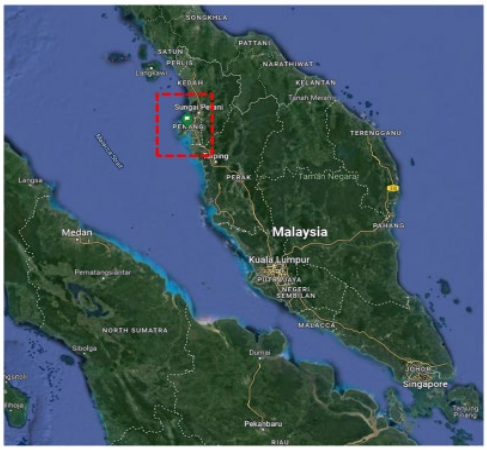

(a) Peninsular Malaysia and Sumatra Island. The red inset shows the location of Penang Island

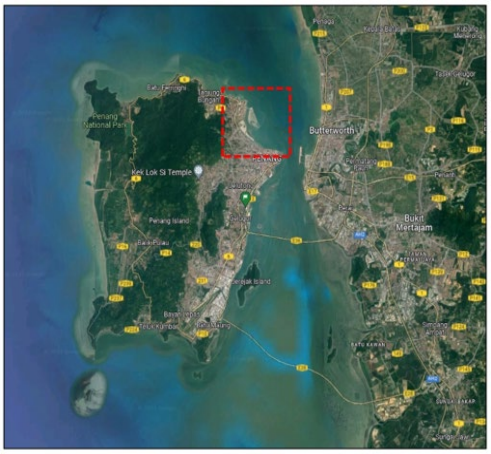

(b) Penang Island. The red inset highlights the location of the STP project

(c) Close up view of the STP project site

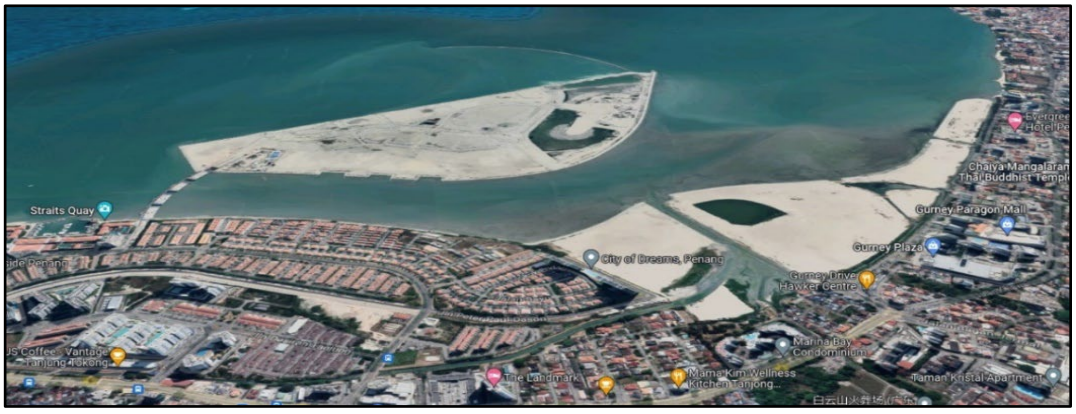

(d) STP2 reclamation project in Penang Island

Figure 1: Google map images showing the Seri Tanjung Pinang (STP) reclamation project.

Land reclamation is a process involving the conversion of an existing or new land from bodies of water by filling it with materials like sand, soil, or concrete. It has been employed for various purposes, including agriculture, housing, and infrastructure construction, dating back to ancient times [3]. However, land reclamation is also associated with adverse effects on the environment, such as soil liquefaction, increased flooding, and pollution of oceans [4],[5]. In recent years, Malaysia has become a prominent player in coastal reclamation projects, with artificial islands being created in multiple states. These projects have resulted in a decline in coastal and marine ecosystem services, elevated costs for restoration efforts, physical displacement, and conflicts between humans and wildlife [6-8]. The local community, particularly fishermen, has also been impacted. Figure 2 provides a visual representation of the changes in the Tanjung Tokong coastline from 1985 to 2020.

Figure 2: Change of coastline at Tanjung Tokong, Penang relamation project from Google Earth (https://earthengine.google.com/timelapse/).

Land reclamation initiatives in Penang began around twenty years ago and continue to be pursued, with plans for future large-scale projects. The Tanjong Tokong land reclamation project is anticipated to have significant effects on coastal evolution, sediment movement, and wave transformation in the surrounding area. It is therefore crucial to comprehend the immediate impact of land reclamation, particularly focusing on the Seri Tanjung Pinang Land Reclamation Project. This is essential for ensuring a sustainable development of the coastal environment by addressing issues related to the coastal evolution, sediment mobility, and wave transformation.

The Seri Tanjung Pinang (STP) is a two-phase development project, in which the first stage of land reclamation, covering 240 acres, was completed in 2006 (referred to as STP1). Subsequently, the second stage involving the reclamation of 760 acres (referred to as STP2) commenced in 2016, and until now, it is still in progress. Previously, the Penang State Government had allocated 20 acres from the initial 240 acres of STP1 for the Penang Outer Ring Road (PORR) alignment [9]. However, these 20 acres will now be part of STP2, resulting in an increased total acreage of STP2 from the original 740 acres (as stated in the Concession Agreement) to 760 acres. In addition to granting rights for land reclamation in STP, the Tanjung Pinang Development (TPD) also independently dredged 131 acres from the Gurney Drive seafront at its own expense, on behalf of the Penang State Government.

Local residents have reported various effects of land reclamation in Malaysia, including physical, biological, socioeconomic, and cultural impacts [10]. One evident physical effect is water pollution, which arises from dredging and sediment removal from the seabed, resulting in water column disturbance and increased siltation [4]. Activities such as sediment transfer between dredging and infilling locations can lead to the release of suspended particles, further contributing to waterway contamination. In specific areas like Tanjung Tokong and Penang National Park in Penang, several reports highlighted increased turbidity, particularly near land reclamation sites [5].

Modelling and calculations of land reclamation activities in Tanjung Tokong, Penang, have revealed observable changes in wave transformation patterns, rates of longshore sediment transport, and subsequent shoreline responses [11]. Following the initiation of the project, sediment transport rates in local areas have significantly altered, resulting in erosion in some regions and sediment accumulation in others. Recent reports have documented infrastructure damage to beach resorts, public gazebos, and watchtowers along the renowned tourist destination of Batu Feringghi, located near Tanjung Tokong, Penang. These damages have been directly attributed to increased erosion and wave surge events along the coastline [5].

Consequently, this research has two primary objectives. Firstly, it aims to comprehend the impact of land reclamation activities on the hydrodynamic conditions in the area, which have been linked to several negative effects on the socio-economic activities of the local population. Secondly, it seeks to investigate the influence of mesh resolution on the hydrodynamic flow surrounding the reclamation site, considering that previous studies (e.g [12], [13], [14], [15]) utilised low mesh resolutions in their numerical models. Ensuring accurate replication of ocean characteristics is of utmost importance to obtain reliable and validated results. To achieve this, the research employs Telemac3D and Acoustic Doppler Current Profiler (ADCP) data at different mesh resolutions to analyse flow variations at the reclamation site. The hope is that the methodology presented in this study can serve as a valuable reference for developing similar models in other reclamation regions.

2. METHODOLOGY

Several tools were employed in the current work, including GEODAS Coastline Extractor, BlueKenue (BK), and Telemac-Macaret modules. The sequential steps undertaken in this research are depicted in Figure 3, commencing with the definition of the study area domain and its importation into BK for pre-processing and preparation for the simulation. Subsequently, the tidal data extracted from TPXO 7.2 - a collection of global ocean tide models, was employed to impose tidal effects on the domain for the purpose of conducting the simulation. The flowchart displays the software used in blue boxes, while the activities performed on the model are represented by orange boxes. The inputs required for the blue boxes are indicated by dotted boxes, as specific inputs are necessary to define the execution of most activities.

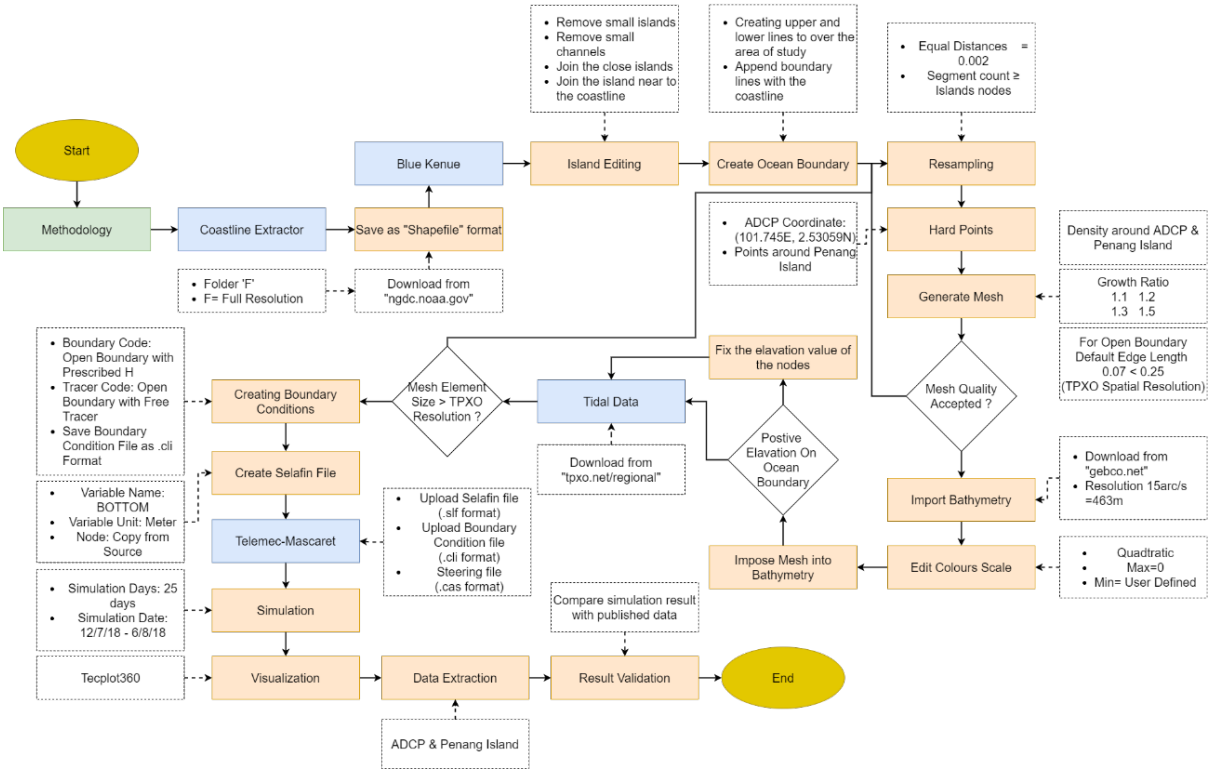

Figure 3: Flowchart illustrating the detailed methodology employed in this study.

2.1 Equations with the hydrostatic pressure assumptions

Telemac, which is an open-source software, utilises a set of assumptions to solve the three-dimensional hydrodynamic equations. These assumptions include the solution of the time-varying Navier-Stokes equations for a free surface, the neglect of density fluctuation in the conservation of mass equation for an incompressible fluid, the application of the hydrostatic pressure hypothesis, and the consideration of the Boussinesq approximation for momentum and density fluctuations under buoyant forces. Based on these assumptions, the module solves the following three-dimensional equations (1) – (5) [12].

$$\frac{\partial U}{\partial x}+\frac{\partial V}{\partial y}+\frac{\partial W}{\partial z}=0 \tag{1}$$

$$\frac{\partial U}{\partial t}+U\frac{\partial U}{\partial x}+V\frac{\partial U}{\partial y}+W\frac{\partial U}{\partial z}=-g\frac{\partial Z_s}{\partial x}+v\Delta(U)+F_x \tag{2}$$

$$\frac{\partial V}{\partial t}+U\frac{\partial V}{\partial x}+V\frac{\partial V}{\partial y}+W\frac{\partial V}{\partial z}=-g\frac{\partial Z_s}{\partial y}+v\Delta(V)+F_y \tag{3}$$

$$p=p_{atm}+p_0g(Z_s-z)+p_0g\int_z^{Z_s}\frac{\Delta\rho}{\rho_0}dz' \tag{4}$$

$$\frac{\partial T}{\partial t}+U\frac{\partial T}{\partial x}+V\frac{\partial T}{\partial y}+W\frac{\partial T}{\partial z}=Div\big(v\,Grad(T)\big)+Q \tag{5}$$

In the equations provided, the following variables are used: Z_s (m) denotes the free surface elevation, U,V,W (m/s) represent the three-dimensional components of velocity, T (0C, g/L...) represents passive or active tracers (which can influence density), p represents pressure, P_{atm} stands for atmospheric pressure, g (m/s^2) represents the acceleration due to gravity, v (m^2/s)

represents the cinematic viscosity and tracer diffusion coefficients, Z_s (m) represents the bottom depth, $\Delta\rho$ represents the variation of density around the reference density, t (s) represents time, x, y (m) represent the horizontal space components, z (m) represents the vertical space component. F_x, F_y (m/s²) represent source terms, and Q (tracer unit) represents tracer sources or sinks. Note that the unknown quantities or computational variables in the equations are h, U, V, W, and T.

2.2 Domain Setup

The initial step in developing the domain involves determining the study area, which in this case is Penang Island. In particular, since the validation data is located in Tanjung Tuan, Negeri Sembilan, the boundaries of the location are extended from Penang to Negeri Sembilan along the Malacca Straits. To establish these boundaries, the Coastline Extractor software was employed, which allows for the inspection, sub-setting, and reformatting of various shoreline files. This software enables the import and export of coasts and borders in different formats. Figure 4 depicts the full-resolution output of the world borders and coasts downloaded from the National Oceanic and Atmospheric Administration (NOAA) website (https://www.noaa.gov).

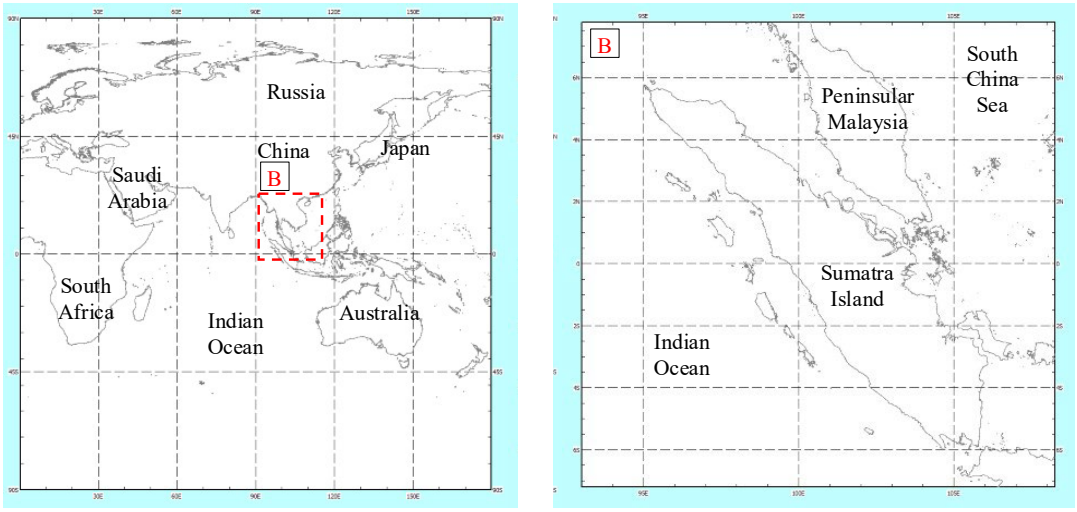

(a) World Map coastline

(b) Coastline focusing on the Sumatra Island and Peninsular Malaysia

Figure 4: Extracted coastline from the tool available on NOAA.

2.2.1 STP Reclamation Site in Penang Island

In order to analyse the impact of reclamation activities on ocean currents near Penang Island, it is necessary to incorporate the coastline of the reclamation project into the model. However, as the STP project is not included in the imported geometry from the coastline extractor, a representation of the STP project area needs to be created. This is accomplished using the Open Line feature in BK, based on the concept layout provided by the Department of Environmental Impact Assessment (DEIA) and reference coordinates from Google Maps.

The Web Plot Digitizer tool was employed to upload the image and set XY coordinates, extracting data points for both the STP1 and STP2 reclamation projects. These data points were then used in BK to construct lines representing the reclamation areas. By appending both models to the coastline, a comparison of Penang Island before and after including the reclamation areas can be observed in Figure 5.

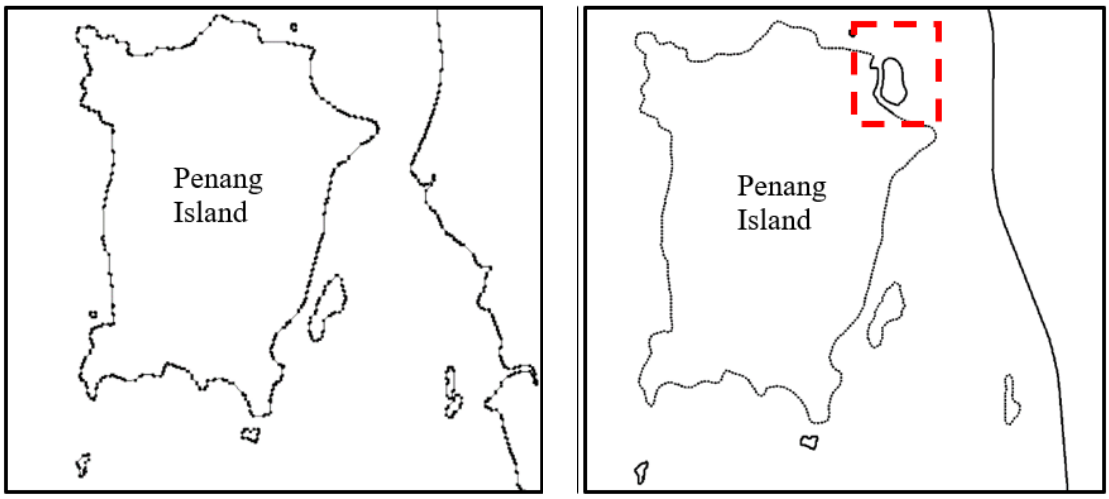

(a) Model coastline before the reclamation activity

(b) Model coastline with the inclusion of the reclamation area (red rectangle)

Figure 5: Comparison of the Penang Island coastline before and after the inclusion of the reclamation area in the model.

2.3 Mesh Generations

Creating an optimal mesh is essential for the accuracy of numerical models. While the quality of the mesh is influenced by various factors, two key parameters play a significant role in any ocean-scale domain development: the mesh edge growth ratio and the default edge length. The mesh edge growth ratio determines the maximum distance by which a mesh element can extend from its neighbouring elements along the boundary. It ensures that the expansion of the element connecting two nodes maintains a specific ratio with the smallest segment on that node. The mesh element size, on the other hand, represents the spacing between each mesh node. In this study, a mesh edge growth ratio of 1.2 was utilised, allowing for a 20% expansion of the elements. It is important to note that the number of elements and nodes within the domain will vary depending on the chosen mesh element size.

The mesh for the Malacca Strait domain, utilised in this study, is depicted in Figure 6. A mesh edge growth ratio of 1.2, the default value in BK software, was employed for this domain. Additionally, the mesh element size was set to 7.77 km. The resulting mesh, shown in Figure 6, consists of 47,329 nodes and 88,328 elements. The figure also illustrates the distribution of elements and nodes along Penang Island and Jerejak Island. The generated mesh for the Malacca Strait, as depicted in Figure 6, serves as a foundation for subsequent steps in model construction. The distribution of the mesh is observable in the image, displaying a structured pattern in the open waters of the strait, devoid of islands. However, as the mesh approaches the islands and coastline, it becomes more irregular to capture the intricate geometry of these landforms. This adaptation of the mesh, with a denser distribution around the islands, was achieved through the resampling process to accurately represent their shapes.

For improved representation of flow propagation near Penang Island and Tanjung Tuan (the validation site), a higher mesh resolution was employed. In Blue Kenue (BK), a closed polygon was used to define a density circle around these specific locations. Within the polygon encompassing Penang Island and the ADCP location, a value was assigned to indicate the desired element size of the mesh, based on published data. By implementing a finer mesh in these areas of interest, the accuracy of data extraction is enhanced.

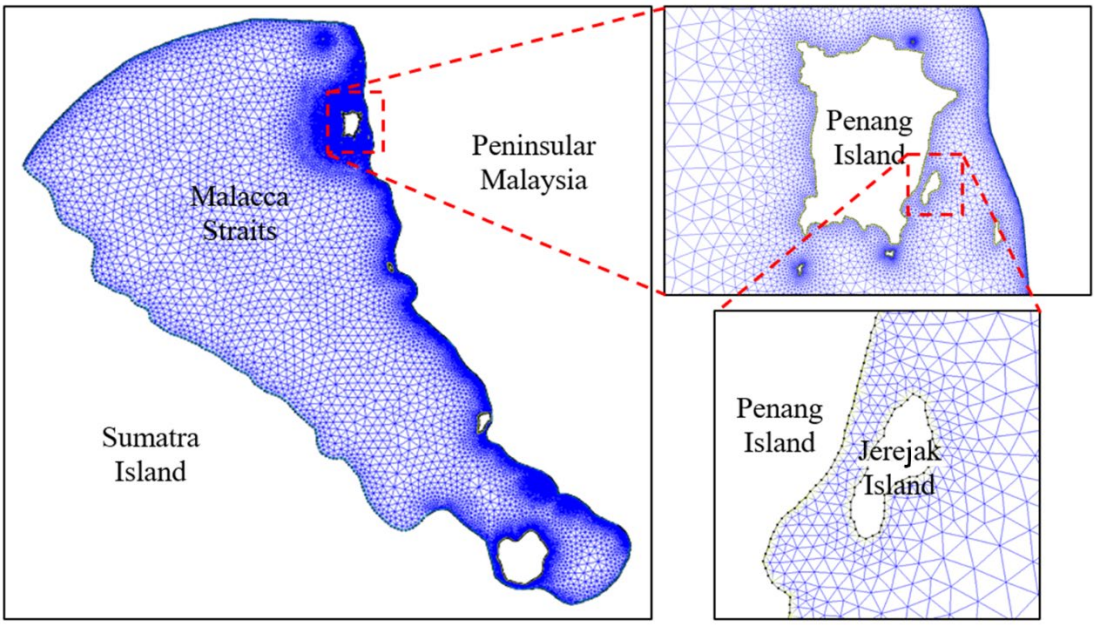

Figure 6: Mesh propagation of the Malacca Strait using the default mesh edge growth ratio of 1.2.

2.3.1 Imposing Bathymetry Data on the Mesh

In hydrodynamic modelling with the Telemac module, the mesh is initialised with zero values at each node. To incorporate bathymetry data from the GEBCO website into the model, the data needs to be downloaded in ASCII format, which is compatible with BK. The available bathymetry data from GEBCO 2022 has a resolution of 15 arc seconds, approximately 463 meters. When selecting the bathymetry boundaries, it is crucial to consider the domain boundaries, such as the Malacca Strait.

The domain boundaries should encompass a larger area than the bathymetry boundaries to avoid elevation values on land areas, such as Sumatra Island and Peninsular Malaysia, which can affect the accuracy of map colours. By adjusting the bathymetry parameters from linear to quadratic, users can modify the maximum value of the bathymetry to address this issue. Setting the maximum value to zero indicates no elevation in the bathymetry, displaying only the ocean portion of the map with depth information. The lowest value of the bathymetry data is approximately -463m, but it may vary in different zones. Figure 7 illustrates the GEBCO 2022 bathymetry data for the Malacca Strait in 3D, with a resolution of 15 arc seconds. It can be seen from the figure that the northern part of the strait exhibits significantly greater depths exceeding 100m, while the rest of the strait has depths below 100m.

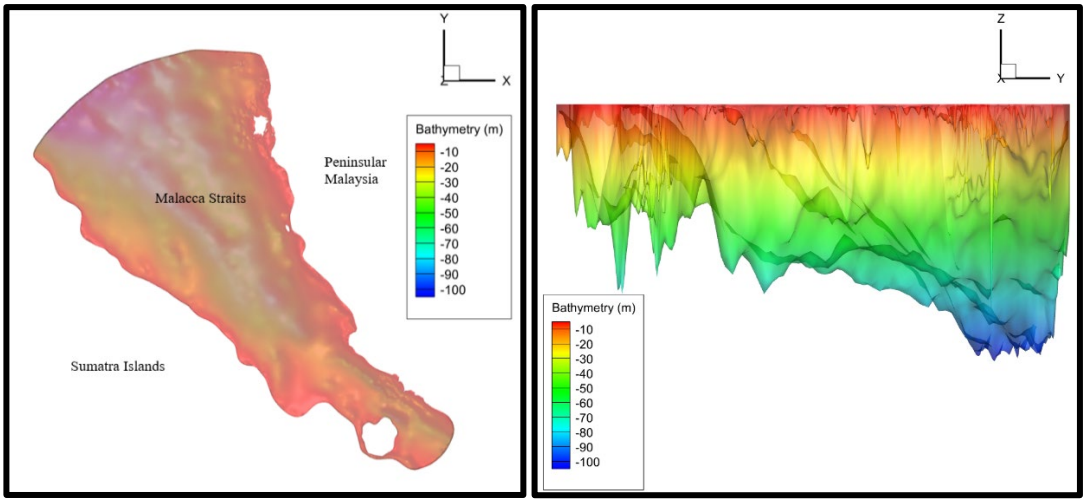

(a) Top View (b) Side View

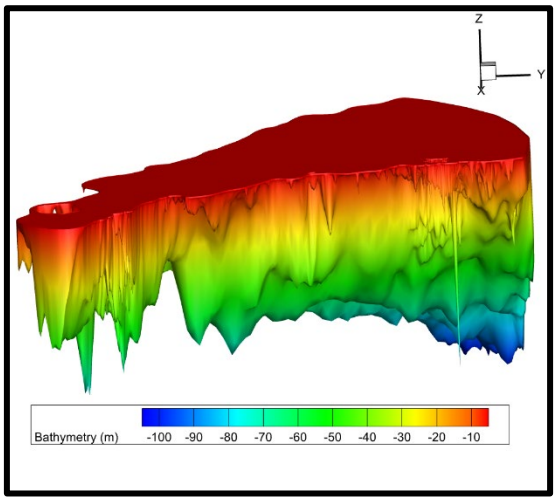

(c) Isometric View

Figure 7: Bathymetry of the Malacca Straits employed in this study.

2.3.2 Fixing Positive Elevations

After applying the bathymetry data to the mesh, some regions along the boundaries may show red and green areas, as depicted in Figure 8. These areas indicate nodes with a depth of zero, while other nodes exhibit positive elevations instead of depths. These discrepancies can be attributed to the limitations in the accuracy of the bathymetry maps used. Despite efforts to ensure precision, small inaccuracies may exist in the data, especially around certain boundaries due to the relatively large spatial resolution of the open-source GEBCO2022 dataset.

To rectify the issue of nodes displaying positive elevations instead of depths, artificial values were assigned to these nodes based on neighbouring nodes. The drawing tools menu was utilised to outline the affected area, creating closed lines that can be assigned artificial values. This process was repeated for each node without depth, with multiple closed lines drawn and assigned false values. The surrounding nodes with positive depths (red) determined the artificial value assigned to the closed lines. In cases where the affected areas were primarily along the shores of islands and coastlines, where node values typically ranged from -1 to -2, a value of -1 was assigned to the majority of the closed lines.

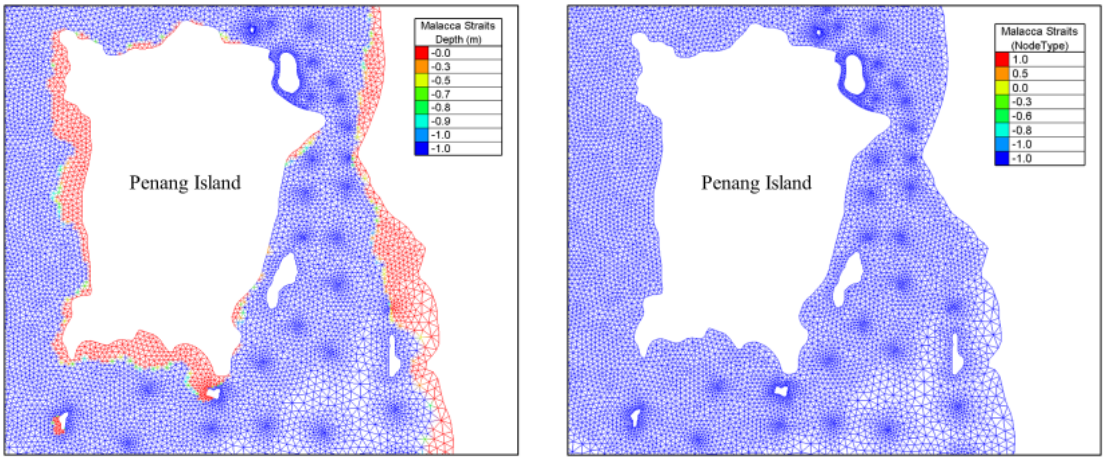

(a) Original mesh with imposed bathymetry (b) Updated mesh with corrected elevation

Figure 8: Illustration of positive elevations when bathymetry is imposed on the model.

2.3.3 Mesh Edge Growth Ratio

The edge growth ratio is a parameter that determines how much a mesh element can expand from its neighbour. A value of 1 signifies no growth, meaning the elements cannot increase in size. Meanwhile, a growth ratio of 1.3, for instance, allows 30% expansion of the elements. Choosing a higher edge growth ratio reduces the number of nodes and elements generated, while a lower ratio creates a denser mesh. In BK, the default edge growth ratio is set to 1.2, allowing for 20% expansion of the elements (see Figure 6). Throughout this study, the default edge length value of 0.07° (equivalent to 7.77 km) was constant for all four different edge growth ratios examined. The smallest ratio employed is 1.1, resulting in crowded elements (Figure 9(a)). Conversely, the highest edge growth ratio used is 1.5, leading to larger elements compared to the smaller ratios (Figure 9(d)).

The selection of mesh parameters in this study was guided by the need to balance computational efficiency with numerical accuracy. Finer meshes generated with lower edge growth ratios provide a more detailed representation of complex coastlines and flow features but demand substantially longer computation times. Conversely, coarser meshes reduce simulation time but may oversimplify local hydrodynamics. The chosen range of edge growth ratios (1.1–1.5) was therefore selected to produce a practical yet sufficiently accurate representation of the coastline geometry in the study area. It should be noted that the optimal range may vary depending on the complexity and scale of other study sites.

Table 1 shows how the edge growth ratio affects the number of nodes and elements in the mesh resolution. Increasing the edge growth ratio from 1.1 to 1.2 resulted in a 40% reduction in the number of elements and nodes compared to the initial value. Similarly, from an edge growth ratio of 1.2 to 1.3, there was a 22% reduction in elements and nodes. When the edge growth ratio was further increased from 1.3 to 1.5, the number of elements and nodes decreased by 20%. Finally, when considering the entire range from an edge growth ratio of 1.1 to 1.5, the number of elements and nodes was reduced by 63%, representing half of the initial count from the edge growth ratio of 1.1.

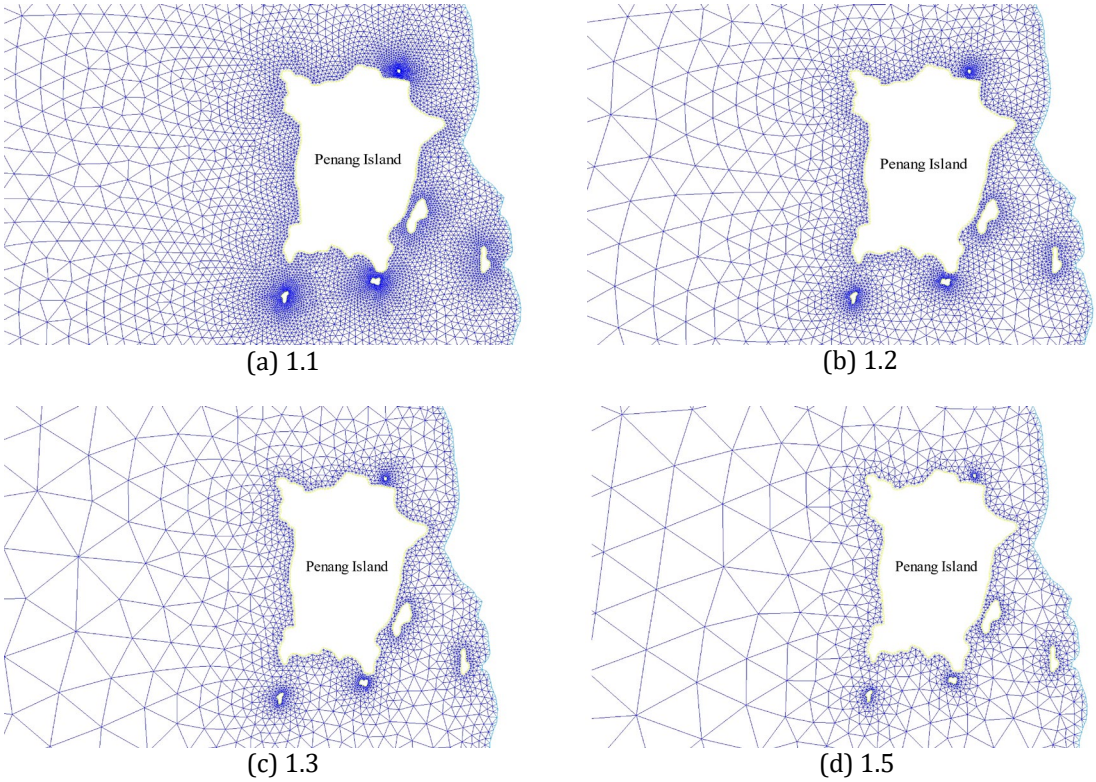

(a) 1.1 (b) 1.2

(c) 1.3 (d) 1.5

Figure 9: Mesh edge growth ratio examined in this study.

Table 1: Nodes & Elements with different edge growth ratios.

Edge Growth Ratio	Nodes	Elements	Percentage Different (%)
1.1	78,439	150,546	-
1.2	47,329	88,328	↓ 40%
1.3	36,782	67,235	↓ 22%
1.5	29,520	52,711	↓ 20%

2.4 Numerical Setup

2.4.1 Boundary Condition

In this study, TPXO is selected as the source for tidal data, offering a comprehensive collection of ocean tidal models that cover global, regional, and local tides [15]. Since the Malacca Strait falls within the Indian Ocean region, the study utilises TPXO's regional data for the Indian Ocean. The resolution of TPXO for the Indian Ocean is 1/12°, corresponding to a spatial resolution of 9.25 kilometres [16]. When importing TPXO tidal data, it is important to consider the element size of the coastline boundary. The distance between each point on the coastline should be smaller than TPXO's element size (9.25 km in this study). Therefore, the resampling process needs to be performed with an element value smaller than TPXO's resolution, following the previously discussed procedures. This ensures the accuracy of the TPXO data, as using larger element sizes may yield unsatisfactory simulation results [17].

To incorporate tidal data into the mesh, boundary conditions (BCs) need to be established. The ocean borders in the north and south of the strait created during the process of defining the ocean boundaries serve as the BCs for the simulation. In the Malacca Strait domain, the BCs are determined by the designated areas or segments where tides enter and exit the domain. These BCs ensure accurate representation of tides in the simulation and allow for the unrestricted flow of water in and out of the Malacca Strait. Figure 10 illustrates the distinct BC imposed on the domain. The Open Boundary with Prescribed H (i.e., water elevation) is represented by a green colour, indicating that tides flow into and out of the domain through these boundaries. In contrast, the rest of the domain is set as Closed Boundary (brown colour), signifying that there is no flow in this region, and the area acts as a solid wall.

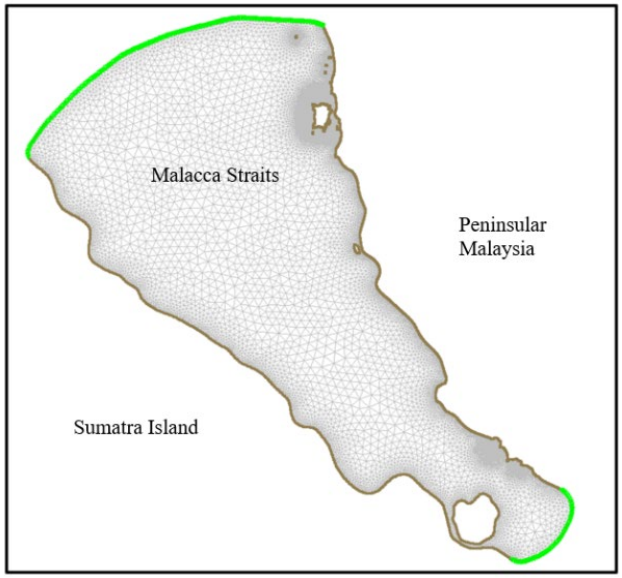

Figure 10: Boundary conditions imposed on the numerical domain used in this study. The Open Boundaries with green line are imposed with water elevation, while the rest of the coastline (in brown) is imposed with a Closed Boundary/wall.

2.4.2 Steering File

To proceed with simulations in Telemac, two files are required from BK: the geometry file and the boundary conditions file. The geometry file, saved in Selafin format (SF), contains detailed information about the mesh created using the bathymetry data. In this study, the variable properties are set to “Bottom” to transfer node values from the bathymetry data to the mesh. The resulting SF mesh, displayed in Figure 11, reveals that the majority of the strait has a depth of less than 200 meters, with the deepest area located in the northwest region of the domain.

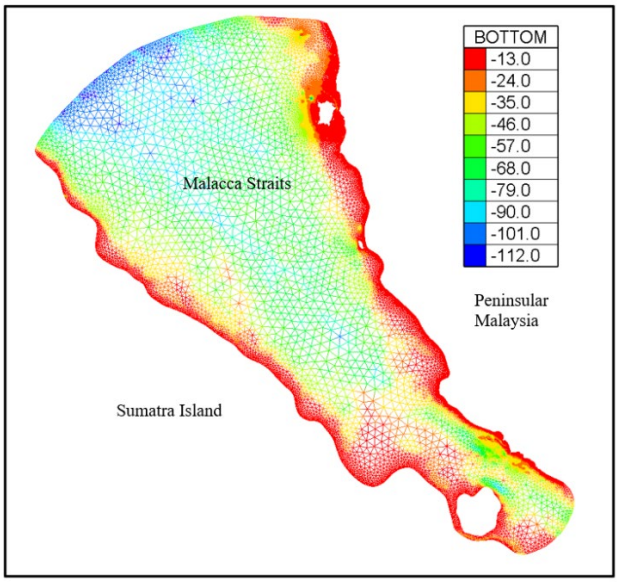

Figure 11: The finalised mesh imposed with the bathymetric dataset for the Malacca Straits in Selafin format.

Telemac3D simulations require four key files: geometry, boundary conditions, steering, and tidal files. The geometry file, in (.slf) format, provides details about the mesh and assigned bathymetry values. The boundary conditions file, in (.cli) format, specifies the characteristics of each boundary. The steering file contains all the necessary information for selecting computational options. Figure 12 illustrates the system dependencies for Telemac3D, covering the entire process from pre-processing to post-processing. Table 2 summarises the mandatory files required for Telemac computations.

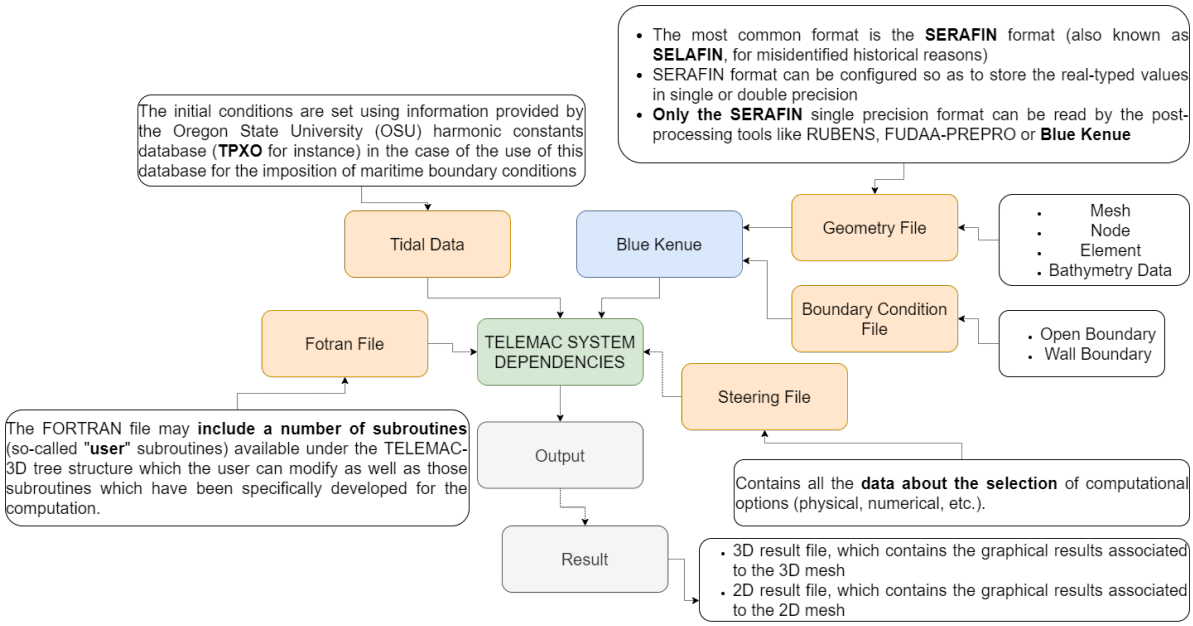

Figure 12: Telemac System Dependencies.

Table 2: Mandatory files for Telemac computation.

File	File format	Descriptions
Geometry file	.slf	Selafin/Seraphin is the generic output and input format of geographical files in the open-source Telemac hydraulic model. This file is in binary format.
Result file		
Boundary condition file	.cli	Containing details of the setting used on each boundary
Steering file	.cas	Contains all numerical configurations for the simulation

In this study, model outputs were recorded at 10-minute intervals, as indicated in Table 3. The geographic system employed for Malaysia was set to UTM zone 47N and the roughness formula used was the Chezy formulation, where the default values were applied for horizontal and vertical viscosity and diffusivity. The vertical and horizontal turbulence models were set to be k-ε, which solves the balance equations for turbulent energy (k) and turbulent dissipation (ε). Notably, using the k-ε model often requires a finer two-dimensional mesh compared to the constant viscosity model, resulting in longer computation times. For this simulation, a device with a 4-core Intel i5 processor and 16 GB of RAM was used. It took approximately 12-13 physical hours to complete the simulation for a single model run, which corresponds to a model duration of 25 days.

Table 3: Numerical parameters for model setup in the steering file.

Numerical parameters	Input/Values
Time step	10 Minutes
Simulation start date	12/07/2018
Simulation period	25 days
Graphic printout period (10 minutes interval)	400 seconds
Law of the bottom friction and friction coefficient	Chezy (90)
Initial condition	TPXO Satellite Altimetry
Option for liquid boundaries	1 (default value)
Tidal database	TPXO 7.2
Horizontal turbulence model	k-ε model
Vertical turbulence model	k-ε model
Number of horizontal levels	3

3. RESULTS & DISCUSSION

3.1 Model Validation

ADCP measurements from a specific site in the Malacca Strait were used to validate the current velocity produced by the models. These measurements were extracted from a study conducted by Goh et al. [18], who conducted a hydrodynamic study near Tanjung Tuan, Negeri Sembilan. The location of the ADCP2 device used in this study is shown in Figure 13, with coordinates of 2.53059N and 101.74538E. Figure 14 shows a reasonable validation and comparison between the two datasets, with slight disagreements expected due to differences in temporal and spatial

resolution. Overall, the trends, peaks, and absence of noticeable phase lags indicate a reasonable match between the model and measurement data.

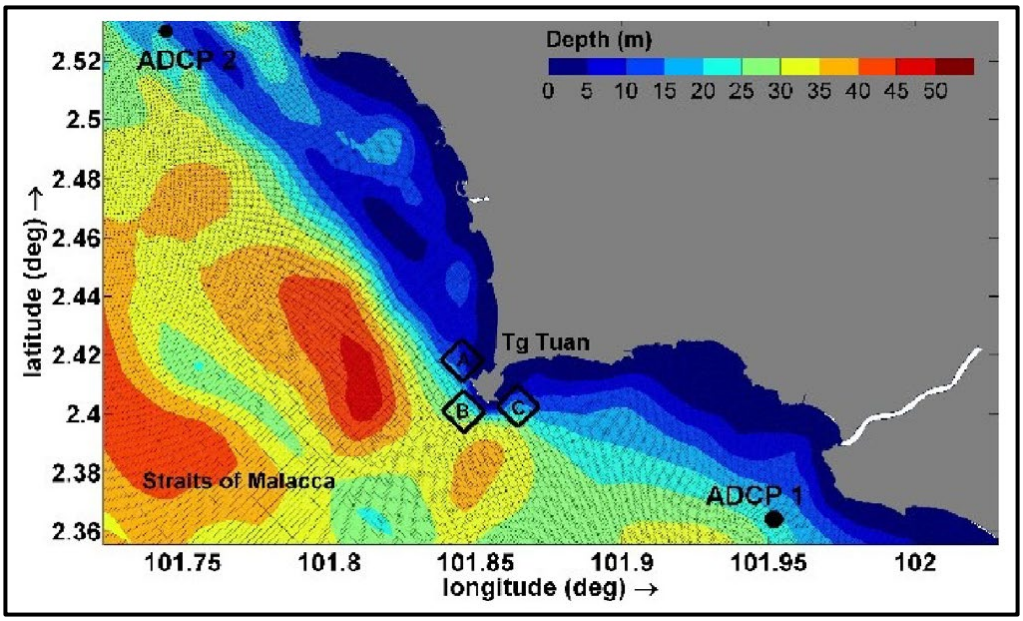

Figure 13: Location of ADCP 1 & 2 that were used by Goh et al [18], and are extracted for this study for validation purposes.

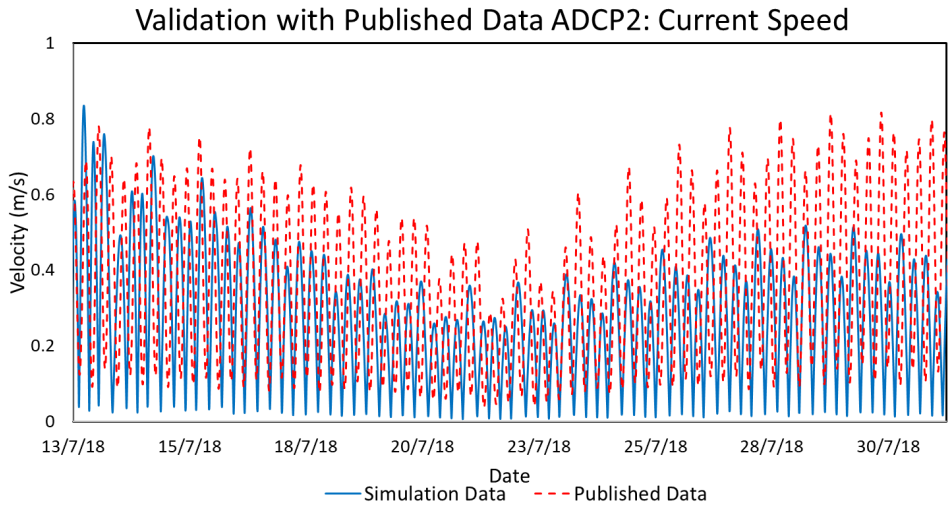

Figure 14: Validation of the predicted current velocity against published ADCP measurement data from [18].

Table 4 compares the simulation data with the published data. The simulation records a maximum velocity of 0.76 m/s, while the published data indicates a maximum velocity of 0.82 m/s, resulting in a difference of 0.06 m/s. The average velocities between July 15th, 2018, and August 6th, 2018, are calculated as 0.26 m/s and 0.37 m/s, respectively, resulting in a difference of 0.11 m/s. The data extraction point corresponds to the ADCP2 location shown in Figure 13. In Figure 14, peaks represent high tides, troughs represent low tides, and the highest and lowest points correspond to spring and neap tides, respectively.

Table 4: Comparison between simulation and published data for the average and maximum velocities at ADCP 2.

Data (m/s)	Predicted / model (m/s)	Published / measured (m/s)	Velocity difference (m/s)
Peak Velocity	0.76	0.82	0.06
Average Velocity	0.26	0.37	0.11

Figure 15 shows the results of tidal velocity magnitude in the Malacca Strait, specifically for high tide conditions, and Figure 21(b) shows the results for low tide conditions. The model assumes the mean tide and utilises the Chezy law with a friction value of 90 for bottom friction. The figure demonstrates that velocity increases near the shorelines where the water depth is shallow, while it decreases in areas farther from the shoreline where the water depth is deeper. Tidal current velocity tends to increase in regions with shorter distances between islands or in narrow areas, such as the lower limit of the Malacca Strait, which becomes narrower as it extends southward. The shallow waters have a greater influence on the lower boundary of the Malacca Strait in terms of tidal current velocity.

Table 5 highlights the selected model for the simulation, which aims to examine the impact of mesh propagation on current speed results. As evident from this table, increasing the edge growth ratio reduces node and element count, resulting in shorter computation time and potential time savings for other models. However, it is crucial to acknowledge that higher edge growth ratios may result in less precise outcomes. Figure 16 displays the results of comparing different edge growth ratios (1.2, 1.3, and 1.5) against published data from Goh et al. [17]. Although all models seem to under-predict the velocity, the overall trend and characteristic of the flow at the measurement site were still managed to be captured by Telemac3D. The underprediction may be attributed to several factors, including uncertainties in bathymetric data resolution, mesh discretization, boundary condition assumptions, and turbulence parameterisation. While this limitation should be noted when interpreting absolute velocity values, the model still provides a sufficiently robust representation of the spatial and temporal hydrodynamic patterns to support the objectives of this study. As expected, the highest velocity is achieved when using an edge growth ratio of 1.2 (i.e., finer mesh propagation), surpassing the velocities obtained with ratios of 1.3 and 1.5 as indicated in Table 6.

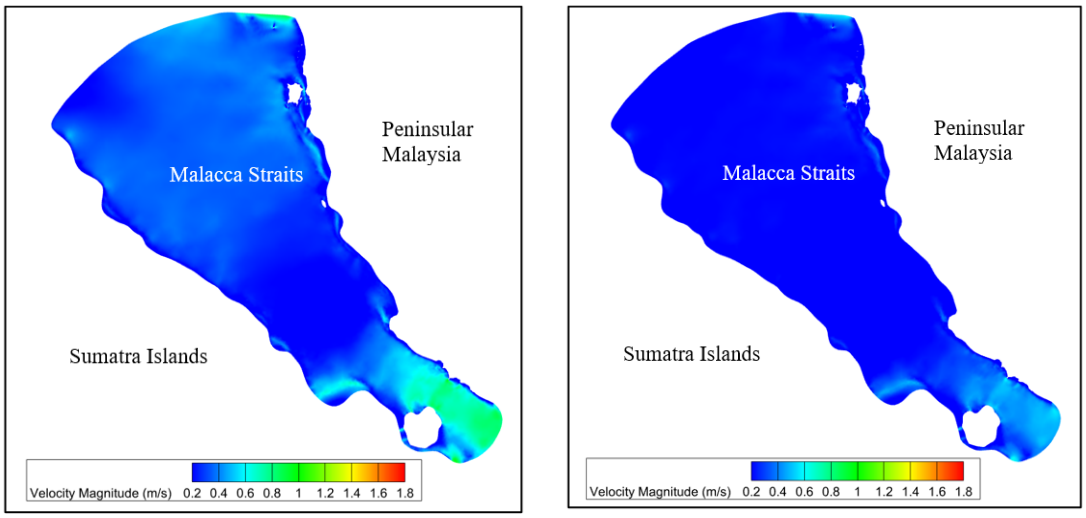

(a) High tide (b) Low tide

Figure 15: Results of velocity magnitude from the simulation using the default numerical setting.

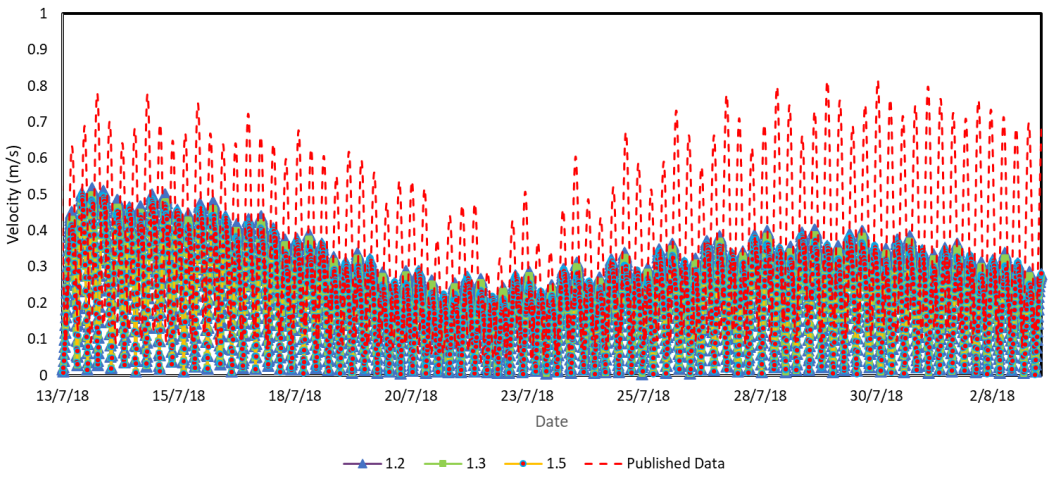

(a) Full simulation period

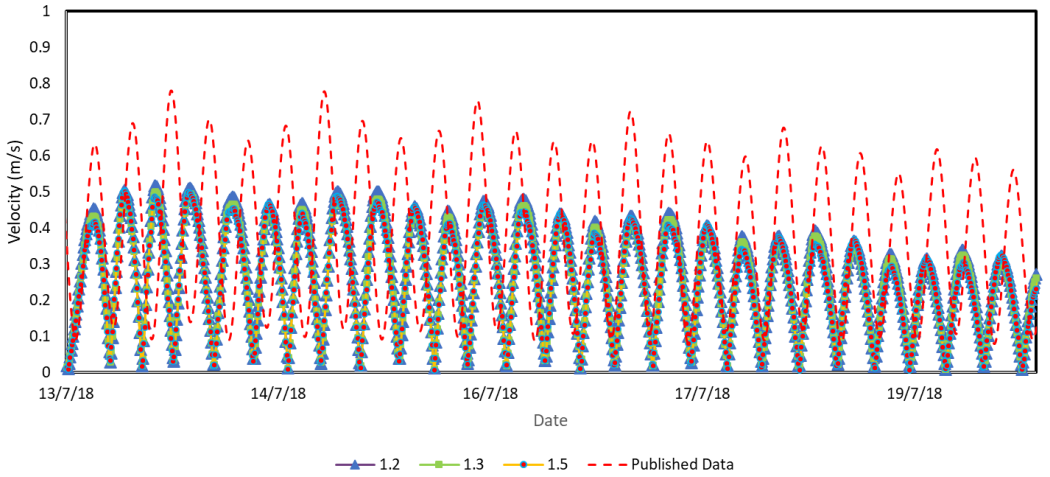

(b) Plot magnification for the first 7 days of the simulation period

Figure 16: Comparison of predicted velocity against measured data for various models with distinct edge growth ratios.

Table 5: Summary of models with distinct edge growth ratios.

Edge Growth Ratio	Default Element Length	Number of Nodes	Number of Elements	Simulation Duration	Simulation Time Step	Computation Time
1.2		26 524	50 511			9 Hours 36 minutes
1.3	0.07	22 045	41 553	25 days	10 minutes printout	8 Hours 10 Minutes
1.5		19 036	35 535			6 Hours 43 minutes

Table 6: Comparison between various edge growth ratios and published data for the average and maximum velocities at ADCP 2.

Data	Edge Growth Ratio			Published Data
	1.2	1.3	1.5	
	m/s			
Peak Velocity	0.51	0.49	0.47	0.82
Average Velocity	0.21	0.20	0.19	0.37

3.1.1 Varying Node Point Values

In addition to applying a finer mesh density over a wide area, BK also provides the ability to control mesh propagation at specific points or nodes. This feature is particularly useful when there is a need to examine or extract data from a precise coordinate within the domain. Figure 17 illustrates how the value assigned to a node influences the propagation of the mesh. In this particular figure, the nodes corresponding to ADCP1 and ADCP2 were assigned values of 0.001 and 0 (default), respectively. It is evident that the mesh propagation around the ADCP1 node is more refined compared to the ADCP2 location, which utilised the default setting. Figure 18 presents the current speed for nodes set to 0 and 0.001 (100m), with ADCP2 serving as the extraction site for data.

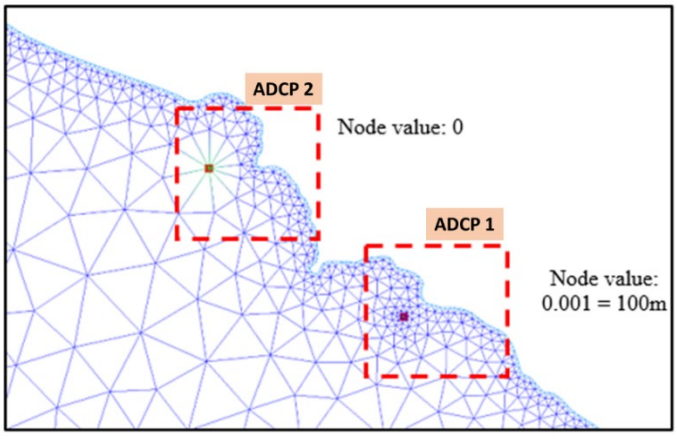

Figure 17: Difference in mesh propagation on node value set up in BK.

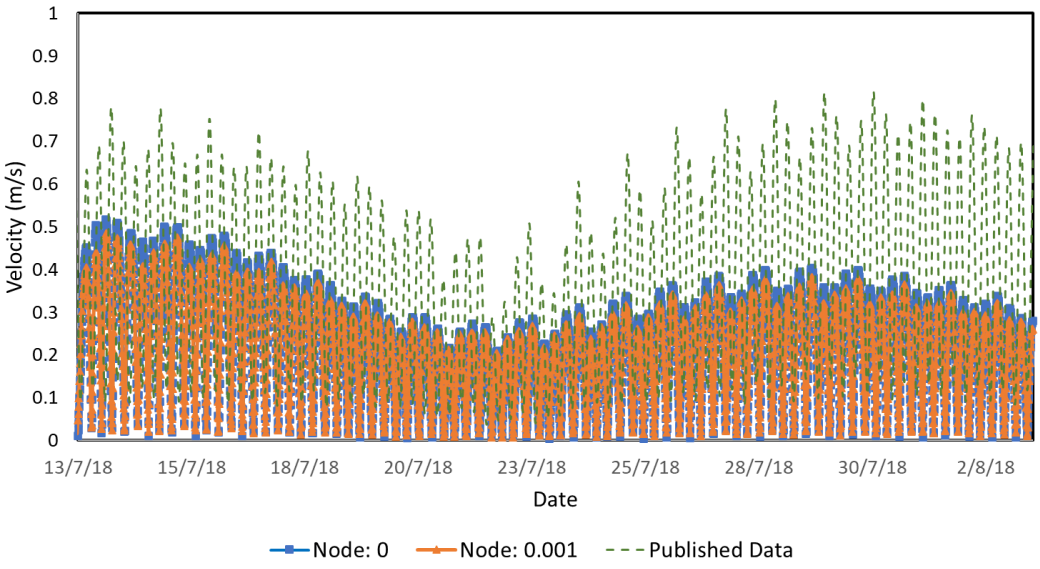

(a) Full simulation period

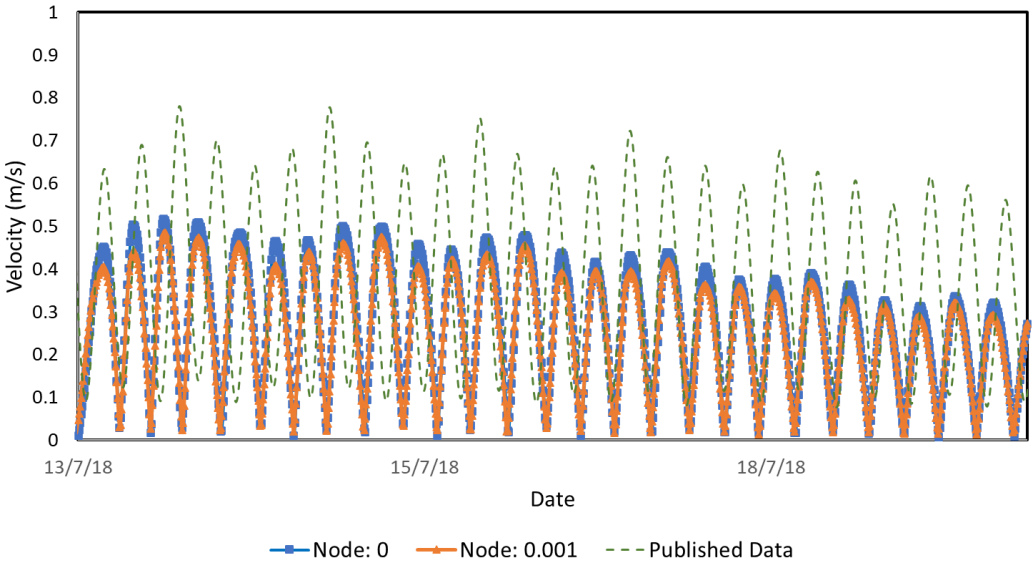

(b) Shorter period comparison

Figure 18: Comparison of predicted velocity against measured data for models with distinct node values.

According to the data in Table 7, when the node value is set to 0, the peak velocity is 0.51 m/s, and the average velocity ranges from 0.21 m/s from July 13th, 2018 to August 4th, 2018. However, when the node value is adjusted to 0.001 (i.e., mesh surrounding the node is around 100 meters), the results show a decrease of 0.03 m/s compared to the previous values, resulting in a current speed of 0.47 m/s. This is because the node with a value of 0.001 experiences greater mesh propagation in its neighbouring nodes, leading to more accurate results compared to the node without a value.

Table 7: Comparison between different node value and published data for the average and maximum velocities at ADCP 2.

Data (m/s)	Node = 0	Node = 0.001	Different in Velocity
Peak Velocity	0.51	0.47	0.03
Average Velocity	0.21	0.20	0.01

3.2 Reclamation Impact on Penang Island

Figure 19 displays the propagation of the mesh around Penang Island, highlighting five nodes that were utilised for data extraction. The first node covers the northern part, the second node is situated in the eastern part, and the third node is located in the south-eastern part of the STP reclamation area. The fourth and fifth nodes are positioned at a certain distance away from the reclamation area to examine the effects of ocean flow. All parameters, including mesh element size, bathymetry data, and coordinates for data extraction, remain unchanged. Table 8 summarises the coordinates, ocean depth, and simulation date for each data extraction point.

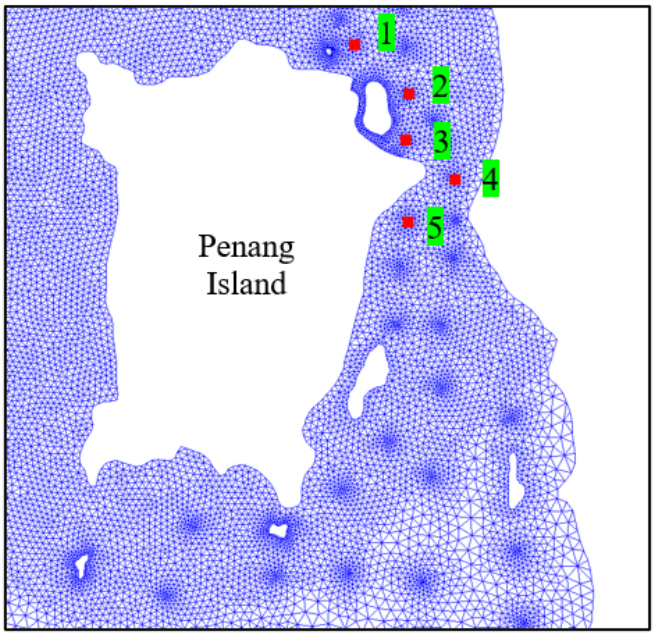

Figure 19: Points used in extracting data around the STP reclamation site.

Table 8: Coordinates of point at reclamation area for data extraction.

Point	Coordinate		Depth (m)	Simulation Date
	Longitude (Deg)	Latitude (Deg)		
1	100.313 E	5.485 N	8	14/7/18 – 5/8/18
2	100.339 E	5.461 N	14	
3	100.338 E	5.439 N	8	
4	100.361 E	5.420 N	8	
5	100.339 E	5.399 N	5	

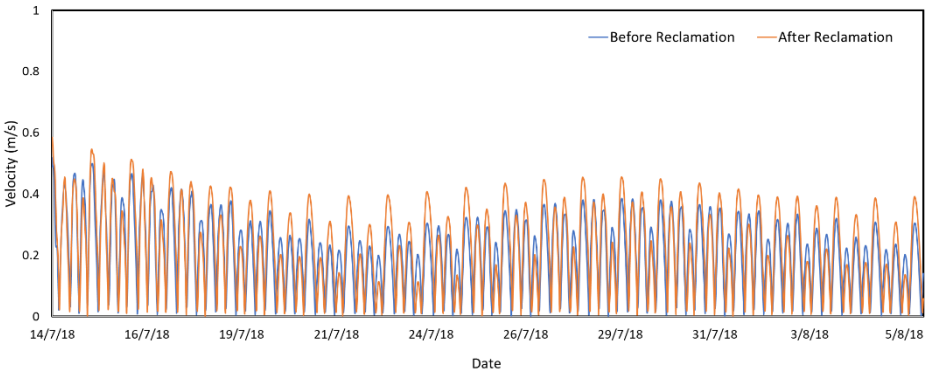

(a) Point 1

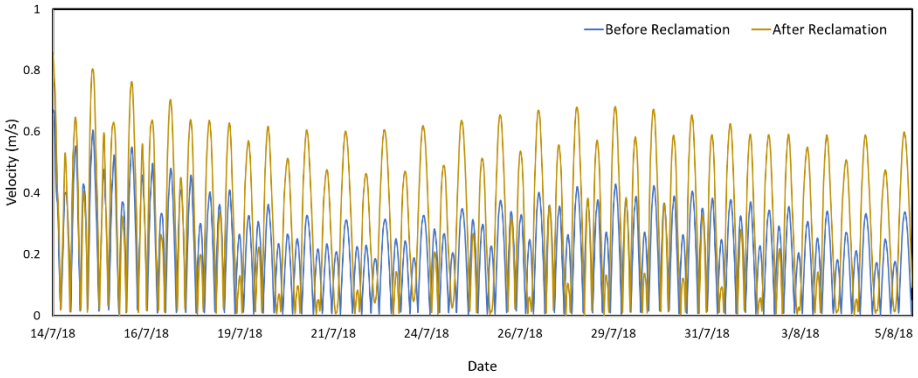

(b) Point 2

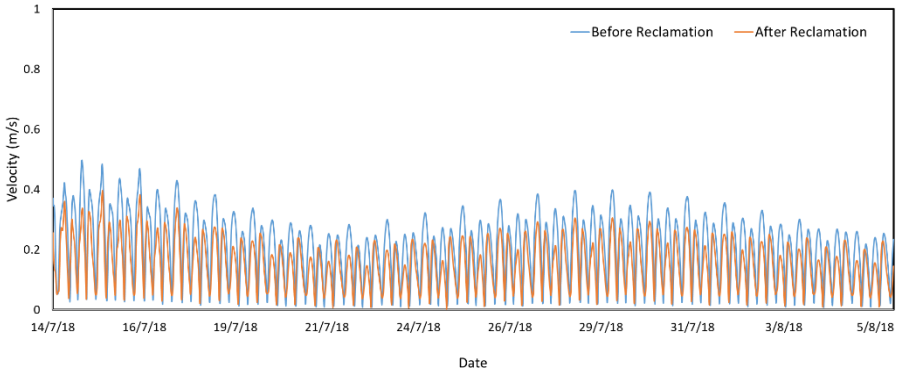

(c) Point 3

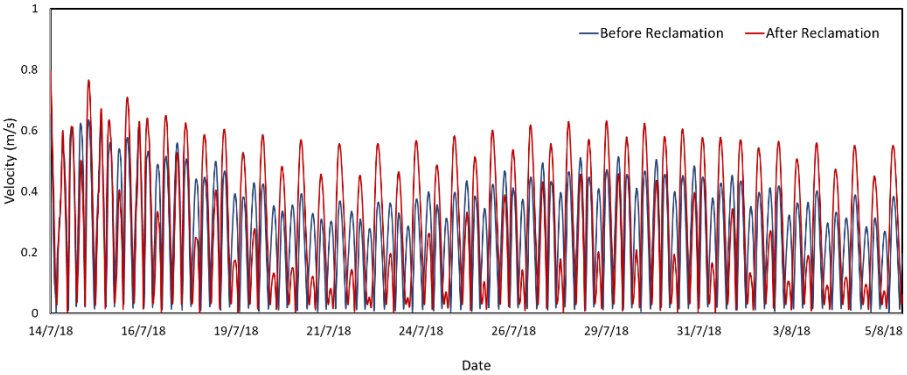

(d) Point 4

Figure 20: Comparison of the reclamation effects on the current speed on Penang Island.

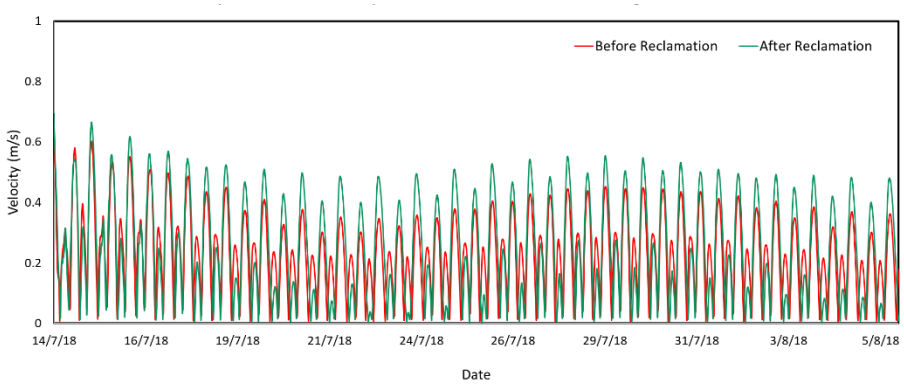

(e) Point 5

Figure 21: Continued.

The simulation results for the current speed are depicted in Figure 20 for each data point highlighted in Figure 19 and Table 8. Additionally, Table 9 provides a comparison of the maximum velocity and average velocity in Penang Island before and after the reclamation activities. Looking at Point 1, the peak velocity before the reclamation activities is 0.52 m/s. After the reclamation activities, the peak velocity increases to 0.59 m/s, resulting in an average change in velocity of 0.07 m/s.

Table 9: Comparison of maximum velocity and average velocity on Penang Island.

Site	Current Speed (m/s)	Before Reclamation	After Reclamation	Change in Velocity
			(m/s)	
Point 1	Peak Velocity	0.52	0.59	0.07
	Average Velocity	0.21	0.22	0.02
Point 2	Peak Velocity	0.67	0.86	0.19
	Average Velocity	0.21	0.31	0.10
Point 3	Peak Velocity	0.50	0.40	-0.10
	Average Velocity	0.21	0.15	-0.05
Point 4	Peak Velocity	0.66	0.79	0.14
	Average Velocity	0.27	0.29	0.02
Point 5	Peak Velocity	0.61	0.69	0.08
	Average Velocity	0.23	0.25	0.02

Moving to Point 2, the peak velocity with reclamation shows an increase from 0.67 m/s to 0.86 m/s. Therefore, the difference after the reclamation activities is 0.19 m/s. However, at Point 3, there is a negative change in velocity. The peak velocity before the reclamation activities is 0.50 m/s, which decreases to 0.40 m/s after the reclamation activities. The negative sign indicates a relative decrease in current velocity compared to the pre-reclamation condition. It is worth noting that Point 2, located in the southern part of the STP reclamation project, experiences wake flow due to the flow of the ocean.

Moving on to Point 4 and Point 5, these points were chosen to examine the flow at a distance from the reclamation projects. At Point 4, there is an increase in the peak velocity from 0.66 m/s before the reclamation activities to 0.79 m/s after the completion of the reclamation works. Similarly, at Point 5, the peak velocity before the reclamation activities rises from 0.61 m/s to 0.69 m/s after

the reclamation activities. These results indicate an overall increase in both maximum and average velocity.

Figure 21 illustrates the current velocity around the STP reclamation area on Penang Island, highlighting a noticeable increase in flow speed and demonstrating the significant influence of reclamation activities on local hydrodynamics. Changes in velocity have far-reaching effects on coastal processes and ecosystems. Higher velocities can enhance sediment transport in some areas while promoting deposition in slower-flow zones, altering seabed morphology, and potentially disrupting benthic habitats. Such changes can reduce the availability of nursery and feeding grounds for fish and other marine species, directly affecting the livelihoods of local fishermen. The footprint of the STP project, combined with sedimentation, may lead to the partial or complete loss of traditional fishing grounds, causing socio-economic challenges for coastal communities.

Furthermore, alterations in flow velocity can intensify coastal erosion in regions with accelerated currents, while areas with slower currents may experience increased sediment accumulation, reshaping the shoreline. These changes can weaken critical habitats such as mangroves and mudflats, which serve as natural barriers against waves and storm surges. The degradation of these ecosystems increases the vulnerability of adjacent agricultural lands to seawater intrusion, which can raise soil salinity and disrupt soil chemistry, reducing suitability for crops sensitive to salinity fluctuations. Overall, the interaction between velocity changes, sediment dynamics, and ecosystem disruption underscores the broader socio-environmental consequences of the reclamation project, affecting both fisheries and the resilience of coastal communities.

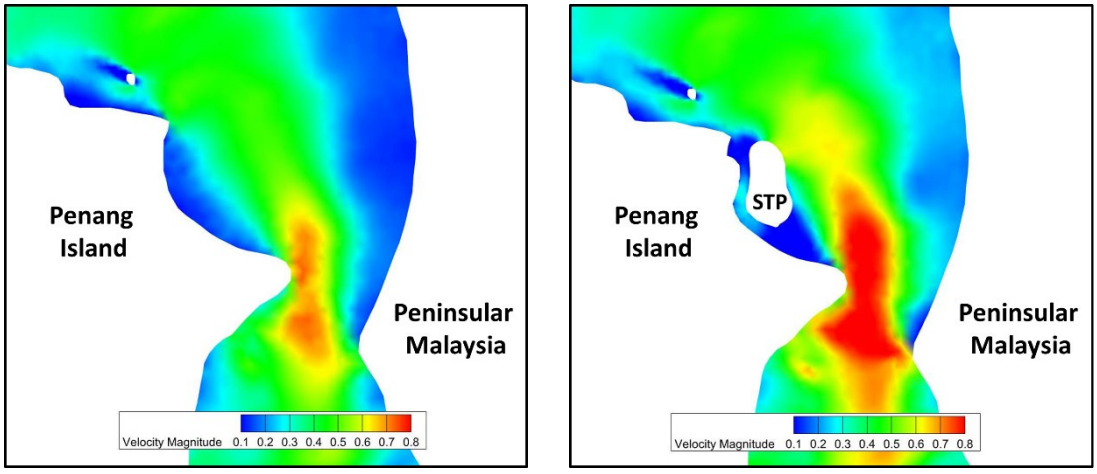

(a) Before the reclamation project (b) After the reclamation project

Figure 22: Visualisation of current velocity in the surrounding reclamation area of Penang Island.

3.3 Factors Affecting Numerical Output

It is worth noting that even an advanced and complex modelling tool such as Telemac3D is still susceptible to errors arising from various factors. These include the spatial resolution of the bathymetry data, the temporal resolution of the measurement dataset, the accuracy of the coastline shape file, the precision of coastline representation, and numerical parameters used in configuring the steering file for computation. One particular factor that can have a significant impact is the size of mesh segments or elements, which influences how the BK software interprets the bathymetry data. Figure 22 provides an example where the bathymetry data is overlaid onto the mesh.

As the bathymetry data is applied to the mesh, the software approximates depth values and assigns them to corresponding mesh elements within the resolution of the bathymetry data, which is depicted as a square shape. This demonstrates the impact of bathymetry resolution and mesh element size on simulation results. When the bathymetry resolution is smaller than the mesh element size, it indicates a higher level of accuracy in the bathymetry data, and vice versa. In the case of the measured data collected by Goh et al [18], the bathymetry data employed is from GEBCO with a resolution of 30 arc seconds, which is approximately 926 meters. This resolution is much lower compared to the bathymetry data used in this investigation by almost half. The bathymetry data employed in this study are sourced from GEBCO 2022 with a resolution of 15 arc seconds, which is equivalent to approximately 463 meters.

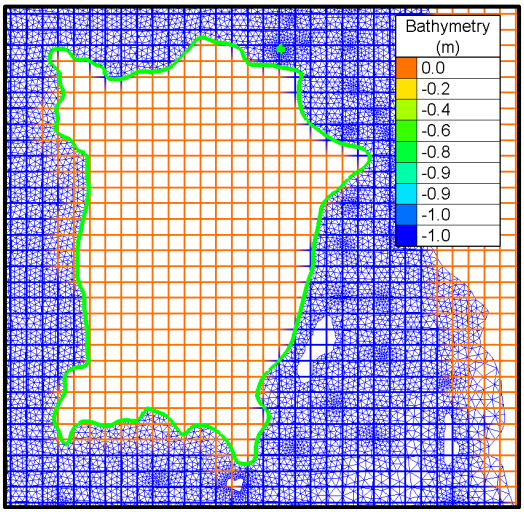

Figure 23: Bathymetry resolution (coloured square-geometry) compared to the coastline of Penang Island (green line).

Furthermore, the accuracy of the coastline data also plays a crucial role in shaping the simulation results by defining the boundary between land and water. In this study, the coastline data is sourced from NOAA. However, it is important to note that the provided shoreline data represents an approximation of the global shorelines. Any modifications made to the coastline (such as resampling and merging of islands) will inevitably alter its original geometry, as illustrated in Figure 23. When combined with other estimated data like GEBCO bathymetry and TPXO data, it can influence the simulation outcomes. Hence, it is important to acknowledge that extreme modifications made to the coastline have severe implications for models' accuracy, particularly if the area of interest is located very close to the coastal area.

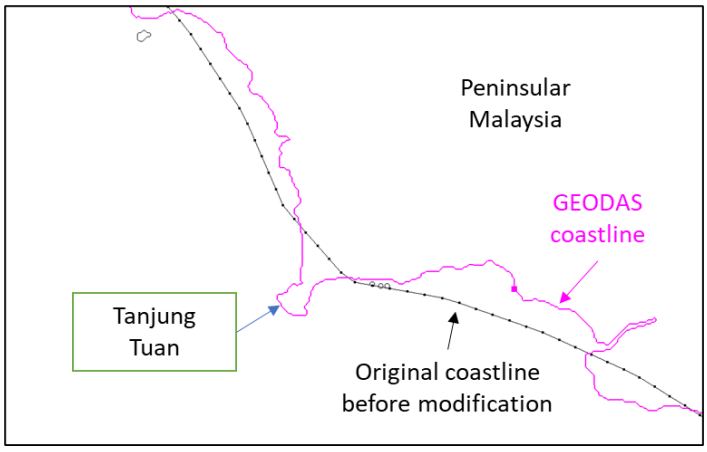

Figure 24: Illustration of the effect of coastline alteration near Tanjung Tuan.

4. CONCLUSION

This study examined the influence of mesh resolution on an ocean-scale hydrodynamics model for Penang Island, using a domain encompassing the entire Malacca Straits to ensure accurate predictions. The results demonstrate that mesh resolution significantly affects tidal velocity, highlighting the importance of high-resolution modelling to capture local-scale flow dynamics and support reliable Environmental Impact Assessments (EIA) for coastal development projects. By testing different edge growth ratios, node distributions, and applied densities, the study confirms that careful selection of mesh parameters is critical to obtain accurate and robust hydrodynamic predictions.

The impacts of reclamation activities around Penang Island were also investigated, revealing notable alterations in local flow patterns. Tidal velocities increased at most measurement points, with potential consequences for both the environment and local communities. Increased sediment transport may adversely affect fisheries, disrupting livelihoods and socio-economic activities. Moreover, critical habitats such as mangroves and mudflats could be degraded as the surrounding environment becomes less suitable for plant growth, particularly for species sensitive to salinity fluctuations. These findings underscore the need for proactive mitigation measures when planning reclamation activities.

Despite these insights, several limitations remain. The bathymetric data used in the model was relatively coarse, which may reduce the accuracy of local-scale velocity predictions, and the model validation was conducted over a short period, limiting the assessment of long-term hydrodynamic variability. To address these limitations, future work could incorporate higher spatial and temporal resolution data to enhance model accuracy and robustness. Expanding the modelling framework to include sediment transport and deposition would allow a more comprehensive assessment of the environmental footprint of reclamation projects. Additionally, considering climate change scenarios could provide valuable insights into potential future impacts on hydrodynamics and coastal ecosystems.

Overall, this study highlights the critical role of high-resolution three-dimensional modelling in understanding the hydrodynamic impacts of land reclamation and provides practical guidance for policymakers to support environmentally informed decision-making and sustainable coastal development.

ACKNOWLEDGEMENTS

The authors would like to extend sincere appreciation for the support given by Universiti Malaysia Perlis (UniMAP), which enabled this research to be carried out.

REFERENCES

[1] Salleh, A. N., et al. Application of geophysical methods to evaluate soil dynamic properties in Penang Island, Malaysia. Journal of Asian Earth Sciences, vol 207 (2021) p. 104659.
[2] Ministry of Environment and Water Malaysia. The proposed reclamation of Sri Tanjung Pinang (phase II), Penang. Detailed environmental impact assessment (Volume 2).
[3] Huang, C., et al. Land reclamation and risk assessment in the coastal zone of China from 2000 to 2010. Regional Studies in Marine Science, vol 39 (2020) p. 101422.
[4] Nadzir, N. M., Ibrahim, M., & Mansor, M. Impacts of Coastal Reclamation to the Quality of Life: Tanjung Tokong Community, Penang. Procedia - Social and Behavioral Sciences, vol 153 (2014) pp. 159–168.

[5] Chee, S. Y., et al. Between the devil and the deep blue sea: Trends, drivers, and impacts of coastal reclamation in Malaysia and way forward. Science of the Total Environment, vol 858 (2023).
[6] Long, A., et al. Implications of European Union recast Renewable Energy Directive sustainability criteria for renewable heat and transport: Case study of willow biomethane in Ireland. Renewable and Sustainable Energy Reviews, vol 150 (2021) p. 111461.
[7] Kinley, R. Climate change after Paris: from turning point to transformation. Climate Policy, vol 17, issue 1 (2017) pp. 9–15.
[8] Tobin, P., Schmidt, N. M., Tosun, J., & Burns, C. Mapping states' Paris climate pledges: Analysing targets and groups at COP 21. Global Environmental Change, vol 48 (2018) pp. 11–21.
[9] Tanjung Pinang Development. Seri Tanjung Pinang (STP) Reclamation Project.
[10] Musa, N. S. N., & Karim, S. A. Q. S. A. Social impact of land reclamation at Seri Tanjung Pinang, Pulau Pinang, Malaysia. 3rd Undergraduate Seminar on Built Environment and Technology 2018 (USBET2018) (2018) pp. 487–491.
[11] Ramly, S. Impact on the coastal areas of the Tanjung Tokong Land Reclamation Project, Penang, Malaysia - Effects on wave transformation, sediment transport, and coastal evolution. Lund University (2008).
[12] Kuşçu Şimşek, Ç., & Arabacı, D. Simulation of the climatic changes around the coastal land reclamation areas using artificial neural networks. Urban Climate, vol 38 (2021) p. 100914.
[13] Kang, C. S., & Kanniah, K. D. Land use and land cover change and its impact on river morphology in Johor River Basin, Malaysia. Journal of Hydrology: Regional Studies, vol 41 (2022) p. 101072.
[14] Wang, X. G., et al. Construction land sprawl and reclamation in the Johor River Estuary of Malaysia since 1973. Ocean & Coastal Management, vol 171 (2019) pp. 87–95.
[15] Goh, H. B., Lai, S. H., Jameel, M., & Teh, H. M. Potential of coastal headlands for tidal energy extraction and the resulting environmental effects along Negeri Sembilan coastlines: A numerical simulation study. Energy, vol 192 (2020) p. 116656.
[16] Oregon State University. OSU TPXO Tide Models - TPXO Global Tidal Solutions.
[17] Rahman, A., & Venugopal, V. Parametric analysis of three dimensional flow models applied to tidal energy sites in Scotland. Estuarine, Coastal and Shelf Science, vol 189 (2017) pp. 17–32.
[18] Goh, H. B., et al. Feasibility assessment of tidal energy extraction at the Tg Tuan coastal headland: A numerical simulation study. Sustainable Energy Technologies and Assessments, vol 38 (2020) p. 100633.

Conflict of interest statement: The authors declare no conflict of interest.

Author contributions statement: Conceptualization and Methodology, Writing & Editing, Anas Abdul Rahman; Investigation, Writing – Original Draft Preparation, Arif Muhamad; Writing & Editing, Ayu Abdul Rahman.